Structure of scavenger receptor SCARF1 and its interaction with lipoproteins

Yuanyuan Wang[1,2,3,§], Fan Xu[1,§],Guangyi Li[4,§], Chen Cheng[1], Bowen Yu[5], Ze Zhang[1], Dandan Kong[1], Fabao Chen[1],Yali Liu[1], Zhen Fang[1], Longxing Cao[6], Yang Yu[4], Yijun Gu[4],Yongning He[1,2,3,7,*]

[1]State Key Laboratory of Oncogenes and Related Genes, Shanghai Cancer Institute, Renji Hospital, Shanghai Jiao Tong University School of Medicine, Shanghai; [2]Shanghai Institute of Biochemistry and Cell Biology, Center for Excellence in Molecular Cell Science, Chinese Academy of Sciences, Shanghai; [3]University of Chinese Academy of Sciences, Beijing, China; [4]National Facility for Protein Science in Shanghai, Shanghai Advanced Research Institute, Chinese Academy of Sciences, Shanghai, China; [5]Department of Immunology, School of Basic Medical Sciences, Weifang Medical University, Weifang, China; [6]School of Life Science, Westlake University, Hangzhou, Zhejiang, China; [7]Department of Biliary-Pancreatic Surgery, Renji Hospital, Shanghai Jiao Tong University School of Medicine, Shanghai, China.

*Correspondence to: Y.H. Email: heyn@shsmu.edu.cn

[§] Equal contributors

Key words: SCARF1; scavenger receptor; lipoproteins; low-density lipoproteins; OxLDL

Abstract

SCARF1 (Scavenger receptor class F member 1, SREC-1 or SR-F1) is a type I transmembrane protein that recognizes multiple endogenous and exogenous ligands such as modified low-density lipoproteins (LDL) and is important for maintaining homeostasis and immunity. But the structural information and the mechanisms of ligand recognition of SCARF1 are largely unavailable. Here we solve the crystal structures of the N-terminal fragments of human SCARF1, which show that SCARF1 forms homodimers and its epidermal growth factor (EGF)-like domains adopt a long-curved conformation. Then we examine the interactions of SCARF1 with lipoproteins and are able to identify a region on SCARF1 for recognizing modified LDLs. The mutagenesis data show that the positively charged residues in the region are crucial for the interaction of SCARF1 with modified LDLs, which is confirmed by making chimeric molecules of SCARF1 and SCARF2. In addition, teichoic acids, a cell wall polymer expressed on the surface of gram-positive bacteria, are able to inhibit the interactions of modified LDLs with SCARF1, suggesting the ligand binding sites of SCARF1 might be shared for some of its scavenging targets. Overall, these results provide mechanistic insights into SCARF1 and its interactions with the ligands, which are important for understanding its physiological roles in homeostasis and the related diseases.

Introduction

Scavenger receptor (SR) was first discovered in late 1970s during the studies regarding the accumulation of low-density lipoprotein (LDL) in macrophages in

atherosclerotic plaques of patients who lack LDL receptors [1, 2]. Up to date, SR family includes a large number of cell surface proteins that can be classified into more than ten classes (class A-L) based on the structural similarities [3]. SRs bind a wide range of endogenous and exogenous ligands including modified lipoproteins, damaged or apoptotic cells and pathogenic microorganisms [4-8] and play important roles in maintaining homeostasis, host defense and immunity, and have been linked to diseases such as cardiovascular diseases, Alzheimer's disease and cancer [9-13].

Scavenger receptor class F (SR-F) has two known members, SCARF1 and SCARF2 [3] (Fig. 1A). SCARF1 was identified in cDNA libraries from human umbilical vein endothelial cells as a receptor for modified LDLs, thus also named SREC-1 (Scavenger Receptors expressed in Endothelial Cells) [14]. It is expressed on the surface of endothelial cells, macrophages, and dendritic cells and distributed in organs such as heart, liver, kidney and spleen [15]. SCARF1 recognizes modified LDLs, including acetylated LDL (AcLDL), oxidized LDL (OxLDL) and carbamylated LDL [14, 16, 17]. Previous studies have shown that the SCARF1-mediated degradation of AcLDL accounts for 60% of the amounts of AcLDL degraded by the pathway independent of scavenger receptor class A (SR-A), suggesting that SCARF1 may play a key role in the development of atherosclerosis in concert with SR-A in some situations [15]. SCARF1 expressed on antigen-presenting cells such as dendritic cells can recognize and internalize heat shock protein-bound antigens and activate adaptive immune responses [18-20]. It may also cooperate with the Toll-like receptors to mediate the cytokine production [7, 21, 22].

SCARF1-knockout mice can develop symptoms similar to systemic lupus erythematosus disease and lead to accumulation of apoptotic cells in the immune organs, suggesting that it is involved in the removal of apoptotic cells and maintaining homeostasis [23]. SCARF1 may also associate with the extravasation of leukocytes from circulation into inflamed tissues during injury or infection, thus having a role in the inflammatory changes in vessel walls and the initiation of atherosclerosis [24, 25]. Recent data also show that SCARF1 is down-regulated in hepatocellular carcinoma and loss of SCARF1 is associated with poorly differentiated tumors [26]. SCARF2 has 35% sequence identity and similar organ distribution with SCARF1 [24]. Genetic analysis suggests that SCARF2 is linked to a rare disease called van den Ende-Gupta syndrome [27, 28], which may provide clues for the physiological roles of this molecule.

Previous reports have shown that SCARF1 can bind a number of endogenous ligands other than modified LDLs, including heat shock proteins [19, 20], calreticulin [29], Ecrg4 [30], Tamm-Horsfall protein [31] and apoptotic cells [23, 32], and mediate ligand internalization and transport [29, 33]. It can also bind bacterial, viral, and fungal antigens [7, 22, 34, 35], but the mechanisms for having such diverse ligand binding properties are unclear. By contrast, SCARF2 shows no binding activity with modified LDLs [24, 36], but recent data suggest SCARF2 may share ligands such as complement C1q and calreticulin with SCARF1 [36]. In addition, MEGF10 (multiple EGF-like domains-10), which might be another member of SR-F family, is a mammalian ortholog of Ced-1 and a receptor of amyloid-β in the brain [13, 37, 38],

suggesting that SR-F family members may have rather wide ligand binding specificities.

SCARF1 (MW, 86 kD) is a type I transmembrane protein that has a short signal peptide followed by a long extracellular region, a transmembrane helix and a large cytoplasmic portion [14] (Fig. 1A). Its ectodomain has three glycosylation sites and contains multiple epidermal growth factor (EGF)-like domains, which usually has a two-stranded β-sheet followed by a loop region and three conserved disulfide bonds [14, 17, 39]. It has been shown that modified LDLs are the ligands for several SRs, including SR-A members, scavenger receptor class B type I (SR-BI), lectin-like oxidized low-density lipoprotein receptor (LOX-1), CD36, etc. [40-43]. For the SR-A members, including SCARA1 (CD204, SR-A1), MARCO and SCARA5, they bind modified LDLs in a Ca^{2+}-dependent manner through the scavenger receptor cysteine-rich (SRCR) domains of the receptors [43]. In the case of LOX-1, both positively charged and non-charged hydrophilic residues might be involved in lipoprotein recognition [44, 45]. And for CD36, positively charged residues are identified to be critical for its binding with OxLDL [46]. Since SCARF1 has different structural features with other known lipoprotein receptors, how it recognizes modified lipoproteins remains unclear.

Here we determined the crystal structures of the N-terminal fragments of SCARF1 and characterized the interaction of SCARF1 with modified LDLs by biochemical and mutagenesis studies, thus providing mechanistic insights into the recognition of lipoproteins by this receptor.

Results

Crystal structures of the N-terminal fragments of SCARF1

To determine the structure of the extracellular region of SCARF1, the intact and several truncation fragments of SCARF1 ectodomain were expressed in insect cells and purified for crystallization screening. Among them, two fragments (f1, 20-132 aa and f2, 20-221 aa) were crystallized and the crystals diffracted to 2.2 Å and 2.6 Å, respectively (Table S1 and S2). The initial phasing for f1 crystal was done by SAD using Pt derivatives and the structure was refined to 2.2 Å with a native dataset after molecular replacement. The crystal of f1 fragment belongs to space group P212121 with two molecules per asymmetric unit (Fig. 1B). The f1 crystal structure contains a number of loops and two stranded β-sheets stabilized by hydrogen bonds and disulfide bonds, which is consistent with the typical feature of EGF-like domains, and it adopts a bow-like conformation with the middle part (~55-102 aa) protruding outwards (Fig. 1B). The electron density of the N-terminal end (~21-62 aa) of one molecule in an asymmetric unit is relatively weak and some residues are missing, probably due to the flexibility of this region.

The structure of f2 fragment was solved by molecular replacement using the structure of f1 fragment combined with the EGF-like fragments predicted by AlphaFold as phasing models and refined to 2.6 Å resolution. The crystal belongs to space group P4122 with one molecule per asymmetric unit (Fig. 1C). In the f2 crystal structure, the N-terminal region of SCARF1 (residue 20-56 aa) and the C-terminal region (210-221 aa) are largely missing, suggesting these regions are quite flexible,

consistent with low electron density of the N-terminal end of the f1 crystal. Rest of the f2 fragment adopts a long-curved conformation with multiple EGF-like domains arranged in tandem (Fig. 1C). Superposition of the two crystal structures reveals the structure of the N-terminal fragment of SCARF1 (20-209 aa) (Fig. 1D), which has similar structural features with the AlphaFold prediction of the molecule (Fig. S1A). However, the crystal structures show a much larger curvature and local differences with the AlphaFold model (Fig. S1A and S2), which is in agreement with a recent report regarding the comparison between the protein structures in PDB and AlphaFold models [47].

SCARF1 forms homodimers

In the crystal of f1 fragment, two molecules in an asymmetric unit are related by a two-fold non-crystallographic symmetry axis. Interestingly, in the crystal of f2 fragment, although an asymmetric unit has only one molecule, the dimer related by the crystallographic two-fold symmetry can be well superimposed with the dimer found in the asymmetric unit of f1 crystals (Fig. 2A), suggesting that dimerization occurs in a similar fashion for the two fragments in different crystal forms. At the dimeric interfaces of f1 and f2 fragments, hydrogen bonds are formed between S88 and Y94 of the monomers, and F82 and Y94 are also close to each other, thus may form π-π interaction (Fig. 2B and 2C). Two salt bridges are also observed in f1 crystals between two monomers, one is between D61 and K71, the other is between R76 and D98 (Fig. 2B).

To further characterize the dimerization of SCARF1, a number of mutants of the

ectodomain were constructed, and the size exclusion chromatography (SEC) was applied to monitor the elution volumes of the proteins. The results showed that mutant S88A, where the hydrogen bonds between S88 and Y94 were removed (Fig. 2C), had a small elution volume shift compared to the wild type (Fig. 2D), suggesting that the homodimers were still maintained, but instability may increase for the dimer. By contrast, mutant Y94A, where the hydrogen bonds and the π-π interactions between Y94 and F82 were both removed, showed a significant elution volume shift (Fig. 2D) and the volume corresponded to the molecular weight of the monomeric SCARF1 ectodomain, suggesting that the π-π interactions between F82 and Y94 were important for dimerization. Other mutants such as S88A/Y94A and F82A/S88A/Y94A also eluted at the volume of the monomer (Fig. 2D). In parallel, we measured the hydrodynamic diameters of the mutants by dynamic light scattering (DLS), and it showed that the wild type and mutant S88A had larger diameters than mutants Y94A, S88A/Y94A and F82A/S88A/Y94A (Fig. 2E), which was consistent with the SEC data. In addition, both the dimeric wild type and the monomeric mutant (S88A/Y94A) of the ectodomain exhibited similar SEC elution volumes at pH 6.0 and pH 8.0, suggesting that pH did not have large impact on the dimerization or the conformation of SCARF1 (Fig. S3).

Interactions of SCARF1 with modified LDLs

To characterize the interaction of SCARF1 with lipoproteins, we monitored the binding of lipoproteins with the SCARF1-transfected HEK293 cells using flow cytometry. The results showed that the SCARF1-transfected cells only bound OxLDL

or AcLDL, rather than native LDL (Fig. 3A), consistent with the previous reports [14, 48], and SCARF1 appeared to have higher affinity for OxLDL than AcLDL (Fig. 3A). In parallel, we also tested the interaction of SCARF1 with high density lipoproteins (HDL) and oxidized HDL (OxHDL), the results showed that both HDL and OxHDL were not able to bind the SCARF1-transfected cells (Fig. 3A). Fluorescent confocal images also confirmed that SCARF1 colocalized with OxLDL or AcLDL, rather than LDL, HDL or OxHDL in the transfected cells (Fig. 3D). Moreover, the flow cytometry data showed that the binding between SCARF1 and modified LDLs occurred either in the presence of Ca^{2+} or EDTA (Fig. 3B-C), suggesting that the interaction of SCARF1 with OxLDL or AcLDL is Ca^{2+}-independent.

To identify the lipoprotein binding region on the ectodomain of SCARF1, we generated a series of truncation mutants, including SCARF1$^{\Delta 20\text{-}132aa}$, SCARF1$^{\Delta 24\text{-}221aa}$, SCARF1$^{\Delta 222\text{-}353aa}$ and SCARF1$^{\Delta 353\text{-}415aa}$ (Fig. 3E). The cells transfected with these mutants were applied to examine the interactions with modified LDLs by flow cytometry. The results showed that the cells transfected with SCARF1$^{\Delta 20\text{-}132aa}$ and SCARF1$^{\Delta 222\text{-}353aa}$ could bind to OxLDL, similar to the cells expressing the wild type (Fig. 3F-G). By contrast, the cells expressing SCARF1$^{\Delta 24\text{-}221aa}$ almost lost binding affinity with OxLDL completely, suggesting that the binding site might locate at the middle region (133-221aa) of the ectodomain of SCARF1 (Fig. 3F). In addition, the cells expressing SCARF1$^{\Delta 353\text{-}415aa}$ showed reduced binding with OxLDL (Fig. 3G), this may not be surprising as the deletion of the C-terminal regions of the ectodomain might change the conformation of the molecule and generate hinderance for the

accessibility of lipoprotein particles.

SCARF1 recognizes modified LDLs through charge interactions

To identify the binding site for modified LDLs on the region identified above (133-221aa), we calculated the surface electrostatic potential of the region based on the crystal structure of f2 fragment [49] and found a positively charged area in this region, which is mainly composed of two sites, one is R160 and R161 (Site 1), the other is R188 and R189 (Site 2) (Fig. 4A). To test whether these positively charged sites are involved in lipoprotein recognition, we generated a number of mutants of SCARF1 including: R160S, R161S and R160S/R161S for Site 1; R188S, R189S and R188S/R189S for Site 2; R160S/R161S/R188S, R160S/R188S/R189S, R160S/R161S/R188S/R189S for both sites, and monitored their binding with OxLDL or AcLDL using flow cytometry. The results showed that all the single mutants for the two sites R160S, R161S, R188S, R189S had similar binding affinities as the wild type (Fig. 4B-C), whereas the two double mutants, R160S/R161S for Site 1 or R188S/R189S for Site 2, exhibited reduced binding affinities with modified LDLs (Fig. 4D-E). And the double mutant for Site 2, R188S/R189S, appeared to have lower affinity than the mutant for Site 1, R160S/R161S (Fig. 4D-E), implying that Site 2, R188S/R189S, may contribute more to the binding. The triple or quadruple mutants, R160S/R161S/R188S, R160S/R188S/R189S and R160S/R161S/R188S/R189S, where positive charges are largely removed for the two sites, almost lost the binding affinities with modified LDLs completely (Fig. 4D-E), suggesting these arginines are crucial for lipoprotein interaction and both sites contribute to the recognition. To

further validate the importance of the charged residues, we made mutants where arginines were substituted with lysines on the two sites, including R160K/R161K, R188K/R189K and R160K/R161K/R188K/R189K. The flow cytometry data showed that all three mutants retained binding activities with modified LDLs (Fig. 4F-G), confirming the importance of charge interactions. Among them, mutants R160K/R161K and R188K/R189K had similar affinities as the wild type, and mutant R160K/R161K/R188K/R189K exhibited a reduction in binding affinity, suggesting the side chains of lysines may be slightly unfavorable for the interactions (Fig. 4F-G). In addition, fluorescent confocal images also confirmed that the mutant R160S/R161S/R188S/R189S did not bind to OxLDL, while the mutants R160K/R161K and R188K/R189K retained binding with OxLDL (Fig. 4H). Taken together, these data suggest that charge interactions are indispensable for the recognition of modified LDLs by SCARF1.

To confirm the binding position identified above for modified LDLs, we expressed and purified the wild type and mutants of the ectodomain of SCARF1 for ELISA (Fig. 5A). The results were consistent with the flow cytometry data, showing that the mutant of the arginines, R160S/R161S/R188S/R189S, lost binding affinity with OxLDL (Fig. 5A). The ELISA data also showed that the monomeric mutants (S88A/Y94A, F82A/S88A/Y94A) had slightly higher affinities with OxLDL than the dimeric wild type, which might be due to the steric hinderance of the dimers when coated onto the plates (Fig. 5A), but flow cytometry suggested that the monomeric mutants had lower affinities than the wide type (Fig. 5B), implying that the dimeric

form may be more efficient to recognize lipoproteins on the cell surface. In addition, we also tested the binding of SCARF1 with OxLDL at pH 6.0 by ELISA and flow cytometry, and both data suggested that the binding activity was retained at pH 6.0 (Fig. 5A and B).

Interactions of modified LDLs with SCARF1/SCARF2 chimeric molecules

As another member in SR-F class, SCARF2 has similar structural features with SCARF1 according to AlphaFold prediction (Fig. S1A-B). However, the flow cytometry data showed that SCARF2 did not bind to AcLDL or OxLDL (Fig. 6A-B), which is in agreement with the previous reports [24, 36]. To further validate the lipoprotein binding sites identified on SCARF1, we generated three pairs of SCARF1/SCARF2 chimeric molecules by switching the counterparts of the two molecules, including: i) SF1-1 and SF2-1, where 1-421aa of SCARF1(ectodomain) and 1-441aa of SCARF2 (ectodomain) are switched; ii) SF1-2 and SF2-2, where 1-221aa of SCARF1 and 1-242aa of SCARF2 are switched; and iii) SF1-3 and SF2-3, where 133-221aa of SCARF1 and 156-242aa of SCARF2 are switched (Fig. 6C-E). Both flow cytometry data and fluorescent confocal images showed that SF2-1 gained binding activity with modified LDL, whereas SF1-1 lost the affinity, suggesting that the ectodomain of SCARF1 is sufficient for lipoprotein interaction (Fig. 6C, 6F-G). Furthermore, the flow cytometry results of SF1-2, SF2-2, SF1-3 and SF2-3 demonstrated that SCARF2 chimeric molecules could bind modified LDLs when its counterparts are replaced by the fragments from SCARF1 that contain the binding sites (Fig. 6D-F), thereby confirming the lipoprotein binding sites identified on

SCARF1. However, the chimeric molecules SF2-2 and SF2-3 showed weaker affinities with OxLDL than SCARF1 or SF2-1 (Fig. 6F), suggesting the overall conformation or residues around the substituted binding region of SCARF2 might also affect ligand interaction. In addition, we made a sequence alignment of SCARF1 from different species and found that the positively charged residues at both site 1 and site 2 are well conserved, but not for SCARF2 (Fig. 6H and Fig. S2), consistent with the importance of these charged residues in ligand recognition for SCARF1.

Interaction of SCARF1 with modified LDLs is inhibited by teichoic acid

Previous reports have shown that SCARF1 has multiple ligands [14, 29-31, 50]. Among them, teichoic acids from *Staphylococcus aureus* has been shown to be able to bind SCARF1 in a charge-dependent manner and mediate adhesion to nasal epithelial cells *in vitro*, and the binding site of teichoic acids locates at the middle region (137-250 aa) of the SCARF1 ectodomain [51]. Here we found that the binding of SCARF1 with OxLDL or AcLDL could be inhibited by teichoic acids efficiently (Fig. 7A-B). And the two double mutants of SCARF1, where the lipoprotein binding sites are mutated, showed more inhibitory effects from teichoic acids (Fig. 7A-B), suggesting that the binding sites for modified LDLs and teichoic acids might be shared or overlapped with each other on the ectodomain of SCARF1.

Discussion

SCARF1 can bind both endogenous and exogenous ligands through its ectodomain [52, 53], which adopts a long-curved conformation with multiple EGF-like domains arranged in tandem according to the crystal structures and the

AlphaFold model. EGF-like domains are commonly found in cell surface molecules [54, 55] and usually bind ligands in a Ca^{2+}-dependent manner [56-58]. The EGF-like domains of SCARF1 do not contain the typical Ca^{2+}-binding sites according to sequence analysis [48] and no obvious Ca^{2+} density is observed in the crystal structures, consistent with the results of biochemical assays, suggesting that the interaction of SCARF1 with modified LDLs is Ca^{2+}-independent. This is in contrast to the SR-A family, where SCARA1, MARCO and SCARA5 bind modified LDLs in a Ca^{2+}-dependent manner [43].

The lipoprotein binding sites of SCARF1 locate at the middle region of the ectodomain and arginines are crucial for recognizing modified LDL by providing positive charges, which may have similarities with WIF-1, a Wnt inhibitory factor containing EGF-like domains that bind glycosaminoglycans through conserved arginines and lysines [59]. In fact, the binding of lipoproteins via charge interactions has been reported before. For LOX-1, which is also a scavenger receptor, positively charged residues such as arginines play essential roles for its binding with OxLDL [44, 45, 60]. And similarly, positively charged residues are important to recognize OxLDL by CD36, which is a member in scavenger receptor class B [46, 61]. Therefore, the interaction of SCARF1 with modified LDLs might be similar to LOX-1 or the SR-B members, rather than the SR-A members. Moreover, both structural and biochemical data suggest that SCARF1 forms homodimers (Fig. 8), which may facilitate the binding of modified lipoproteins and is also analogous to some of the lipoprotein receptors such as LOX-1[62, 63].

Among the ligands of SCARF1, the teichoic acids from *Staphylococcus aureus* have been shown to interact with SCARF1 in a charge-dependent manner [51], which is similar to modified LDLs that also need charged residues to bind SCARF1. Therefore, teichoic acids and modified LDLs may share the binding sites on the ectodomain of SCARF1, implying that this region might be a general binding position for some of the scavenging targets, but whether all the ligands utilize this region for binding needs further investigation. In addition, the sequence alignment also shows that these charged residues are well conserved in different species for SCARF1, but SCARF2 lacks such sites on the ectodomain (Fig. S2), suggesting SCARF1 and SCARF2 are functionally divergent, although they have some sequence similarities.

Over the past decades, SCARF1 has been linked to a number of diseases, including cardiovascular diseases, systemic lupus erythematosus, fungal keratitis and cancer [26, 32, 53, 64]. But the mechanisms and roles of SCARF1 in these diseases are largely elusive. The structural and mechanistic characterization of SCARF1 and its interactions of multiple ligands would shed light on the physiological and pathological roles of this receptor on the corresponding pathways and may also provide insights on the therapeutic strategies against the related diseases.

Materials and methods

Protein expression and purification

For protein expression in insect cells, the cDNA of human SCARF1 encoding f1 (20-132aa) and f2 (20-221aa) fragments were sub-cloned into a pFastBac vector fused with an N-terminal melittin signal peptide and a C-terminal 6xHis tag using NovoRec

recombinant enzyme. Sf9 cells were used for generating recombinant baculoviruses and high five cells were used for protein production. The infected cells were cultured in ESF921 medium (Expression Systems) for 3 days in a 27°C humidified incubator. The supernatants were buffer-exchanged with 25 mM Tris, 150 mM NaCl at pH 8.0 by dialysis, then applied to Ni-NTA chromatography (Ni-NTA Superflow, Qiagen). The eluted proteins were concentrated to 1 ml using Amicon Ultra-15 3k-cutoff filter (Millipore) and loaded onto a HiLoad Superdex 75 prep grade column (GE Healthcare) with Tris-NaCl buffer (10 mM Tris, 150 mM NaCl at pH 7.5) for further purification. The purified proteins were loaded onto SDS-PAGE (12%) and stained with coomassie brilliant blue R250 for detection.

For protein expression in mammalian cells, the cDNAs of the human SCARF1 ectodomain and mutants (S88A,Y94A,F82A/S88A,S88A/Y94A,F82A/S88A/Y94A) were sub-cloned into a pTT5 vector fused with a C-terminal 6xHis tag. The transfected HEK293F cells were cultured in suspension for 5 days in a CO_2 humidified incubator at 37°C, then the supernatants were collected and applied to Ni Smart Beads (Smart-lifesciences). The eluted proteins were concentrated to 1 ml using Amicon Ultra-15 10k-cutoff filter (Millipore) and loaded onto a HiLoad Superdex 200 prep grade column (GE Healthcare) with Tris-NaCl buffer (50 mM Tris, 150 mM NaCl at pH 8.0) for further purification. The purified proteins were loaded onto SDS-PAGE (10%) and stained with coomassie brilliant blue R250 for detection.

Cell culture and transfection

HEK293T cells were cultured in Dulbecco's modified Eagle's medium

(HyClone) supplemented with 10% fetal bovine serum and cells were incubated in a humidified incubator at 37 °C with 5% CO_2. The cells were seeded in a 12-well plate in advance, and on the day of transfection, the cells that were 80%-90% confluent in the 12-well plate were transfected using PEI (Polyplus). After 4-6 h of transfection, the culture medium was replaced by the fresh medium. Then about 24 h after transfection, the cells were ready for assays.

HEK293F cells were cultured in suspension with Union-293 medium (Union Bio) in a humidified incubator at 37 °C with 8% CO_2. Transfections were done at the cell density of 1.5-2.0$\times 10^6$/ml using PEI (Polyplus) and after 24 h, the cells were ready for assays.

Crystallization and structural determination

The purified protein was concentrated to 30 mg/ml (f1, 20-132aa) and 10 mg/ml (f2, 20-221aa) (measured by UV absorption at 280nm) using Amicon Ultra-15 3k-cutoff filter (Millipore). Crystal screening was done at 18 °C by sitting-drop vapor diffusion method using 96-well plates (Swissci) with commercial screening kits (Hampton Research). A Mosquito nanoliter robot (TTP Labtech) was used to set up 200 nl protein sample mixed with 200 nl reservoir solution. The crystals of f1 were grown in a solution containing 20% (w/v) polyethylene glycol 3350, 0.2 M ammonium sulfate, 0.1 M Bis-Tris (pH 5.5) and the crystals of f2 were grown in 0.1 M citric acid/sodium citrate (pH 3.6), 0.2 M sodium citrate tribasic, 9% PEG6000. Crystals of both fragments were obtained after 5-7 days. 10% ethylene glycol was added during crystal harvest and data collection as cryo-protectant. The f1 crystal

heavy atom derivatives were obtained by soaking with 10 mM K_2PtCl_4 for 2 minutes before data collection. Diffraction data were collected using a PILATUS 6M detector at BL18U1 beamline of National Facility for Protein Science Shanghai (NFPS) at Shanghai Synchrotron Radiation Facility (SSRF). X-ray diffraction data were integrated and scaled with HKL-3000 package [65].

The initial phasing of the f1 crystals was done by SAD with Pt derivatives, then molecular replacement was done with a native data set of f1. The f2 crystal structure was solved by molecular replacement using the structure of f1 fragment combined with the EGF-like fragment predicted by AlphaFold as search models using Phenix [66, 67]. Model building and refinement were done using Coot [68] and Phenix [69, 70]. The structural figures were prepared using UCSF Chimera [71]. The coordinates and the structure factors have been deposited in the Protein Data Bank with entry 8HN0 and 8HNA for f1 and f2 fragments, respectively.

Mutagenesis experiments

SCARF1 mutations, including base-substitution mutations (R160S, R161S, R188S, R189S, R160S/R161S, R188S/R189S, R160K/R161K, R188K/R189K, R160S/R161S/R188S, R160S/R188S/R189S, R160S/R161S/R188S/R189S, R160K/R161K/R188K/R189K,S88A,Y94A, S88A/Y94A, F82A/S88A/Y94A), deletion mutations ($SCARF1^{\Delta 20\text{-}132aa}$, $SCARF1^{\Delta 24\text{-}221aa}$, $SCARF1^{\Delta 222\text{-}353aa}$, $SCARF1^{\Delta 353\text{-}415aa}$) were introduced into the corresponding plasmids by PCR using KOD DNA polymerase (Sparkjade Science Co., Ltd.). The template plasmids were digested by DpnI (Thermo Fisher Scientific), and the digested PCR products were

ligated by Ligation High (TOYOBO). The chimeric molecules of SCARF1 and SCARF2 were constructed by replacing fragments (1-441aa, 1-242aa, or 156-242aa) of SCARF2 with its counterparts of SCARF1 (1-421aa, 1-221aa or 133-221aa), respectively.

Dynamic Light Scattering

The purified protein samples were concentrated to about 100 μg/mL in Tris buffer (50 mM Tris, 150 mM NaCl at pH 8.0) and dynamic light scattering signals were measured and processed on a Zetasizer Pro analyzer (Malvern Panalytical). Data for each sample were collected in triplicate at 25°C.

Preparation of modified lipoproteins

Lipoproteins (purity, 97%-98%), including Dil-LDL (20614ES76), Dil-AcLDL (20606ES76), Dil-OxLDL (20609ES76), LDL (20613ES05), AcLDL (20604ES05) were purchased from Yeasen. Dil-HDL (H8910) was purchased from Solarbio. The lipoproteins mentioned above (LDL, AcLDL, OxLDL, HDL) were isolated from human plasma.

For preparation of OxHDL, 140 μl of 1 mg/ml HDL were buffer-exchanged to PBS solution, and then the same volume of 100 μM $CuSO_4$ was divided into multiple small portions and added to HDL solutions gradually. After 16 h at 37°C, the reaction solutions were dialyzed against the PBS buffer containing 0.3 mM EDTA to stop the reaction.

Flow cytometry

For the binding assays of SCARF1 and SCARF2 with lipoproteins, HEK293T

cells were transiently transfected with the full-length SCARF1 or SCARF2 fused with a C-terminal GFP tag. After 24 h, 5 μg Dil-tagged (wavelength: 565 nm) lipoprotein (Dil-LDL, Dil-AcLDL, Dil-OxLDL, Dil-HDL, Dil-OxHDL) was added to the culture medium. After 2 to 4 h at 37°C, cells were washed three times with the washing buffer (25 mM Hepes, 150 mM NaCl, 0.1% Tween 20, pH 7.4) and then washed twice with the cleaning buffer (25 mM Hepes, 150 mM NaCl, pH 7.4) for flow cytometry.

For the Ca^{2+} assays, HEK293T cells were transiently transfected with the full-length SCARF1 fused with a C-terminal GFP tag. After 24 h, 5 μg Dil-labeled lipoprotein (Dil-AcLDL, Dil-OxLDL) was added to the culture medium containing 2 mM Ca^{2+} or 2 mM EDTA. After 2 to 4 h, the cells were washed twice with the corresponding washing buffer (25 mM Hepes, 150 mM NaCl, 0.1% Tween 20, 2 mM Ca^{2+}, or 2 mM EDTA, pH 7.4) and then washed twice with the cleaning buffer (25 mM Hepes, 150 mM NaCl, 2 mM Ca^{2+}, or 2 mM EDTA, pH 7.4) for flow cytometry.

For the binding assays of the SCARF1 mutants with lipoproteins, HEK293T cells were transiently transfected with the wild type or the mutants of SCARF1 fused with a C-terminal GFP tag. After 24 h, 5 μg Dil-tagged (wavelength: 565 nm) lipoprotein (Dil-LDL, Dil-AcLDL, Dil-OxLDL) was added to the culture medium. After 2 to 4 h at 37°C, cells were washed three times with the washing buffer (25 mM Hepes, 150 mM NaCl, 0.1% Tween 20, pH 7.4) and then washed twice with the cleaning buffer (25 mM Hepes, 150 mM NaCl, pH 7.4) for flow cytometry. For the assays performed at pH 6.0, PBS buffer (pH 6.0) was used following the similar

procedure.

For the assays to monitor the expression of SCARF1 and mutants, HEK293F cells were transiently transfected with the wild type or the mutants fused with a C-terminal GFP tag. After 24 h, Human SREC-I/SCARF1 Alexa Fluor 647-conjugated Antibody (FAB2409R, R&B SYSTEMS) was added to the culture medium. After incubation of 30 min at 4°C, cells were washed three times with the washing buffer (135 mM NaCl, 2.7 mM KCl, 1.5 mM KH_2PO4, and 8 mM K_2HPO4) for flow cytometry (Fig. S4).

Flow cytometry data were acquired using a LSR Fortessa flow cytometer (BD Biosciences). Data analysis was performed using FlowJo software (Tree Star, Inc).

ELISA experiments

Lipoprotein (OxLDL) was coated onto 96-well plates with 1 μg protein per well at 4 °C overnight. The plates were then blocked with the blocking buffer (25mM Hepes,150mM Nacl,0.1% Triton X-100,and 5%(w/v) BSA, pH 7.4) at room temperature for 3 h. The purified His-tagged proteins was serially diluted and added to each well in the binding buffer (25mM Hepes,150mM Nacl,0.1% Triton X-100,and 2 mg/ml BSA, pH 7.4). After incubation at room temperature for 2 h, the plates were washed five times with the washing buffer (25mM Hepes,150mM NaCl and 0.1% Triton X-100, pH 7.4) and then incubated with the mouse anti-His antibody (66005-1-Ig, Proteintech) for 1 h. After washing three times with the washing buffer, the plates were incubated with the HRP-labeled goat anti-mouse IgG (A0216, Beyotime) for 1 h. After washing three times with the washing buffer, 100 μl TMB

Chromogen Solution (P0209-500ml, Beyotime) was added to each well and incubated for 30 min at room temperature. Then, 50 μl H_2SO_4 (2.0M) was added to each well to stop the reactions. For the binding of lipoproteins at pH 6.0, PBS buffer (pH 6.0) was used following the similar procedure. The plates were then read at 450nm on a Synergy2 machine (Bio Tek Instruments).

Confocal microscopy

HEK293T cells were grown on coverslips and transfected with the full-length SCARF1, SCARF2 or the mutants of SCARF1 fused with a C-terminal GFP tag using 6-well plates. After 24 h of transfection, 5 μg Dil-labeled Lipoprotein (Dil-LDL, Dil-AcLDL, Dil-OxLDL, Dil-OxHDL) added to the plates. After 2 to 4 h of incubation, the cells were fixed by 4% paraformaldehyde in TBS (50 mM Tris and 150 mM NaCl, pH7.4). After washing twice with the buffer (25 mM Hepes, 150 mM NaCl, 0.05% Tween-20, pH 7.4). Then the cells were blocked in the blocking buffer (25 mM Hepes, 150 mM NaCl, 5% (w/v) BSA, 0.05% Tween-20, pH7.4) at room temperature for 1 h. After washing three times with the washing buffer (25 mM Hepes, 150 mM NaCl, 0.05% Tween-20, pH 7.4) and the cells were incubated with 5 μM DAPI for 15 min. Then the plates were washed again for confocal microscopy with a Leica SP8 microscope.

Data availability

The crystal structures of the human SCARF1 fragments, f1 and f2, are deposited in PDB (www.rcsb.org) with entry 8HN0 and 8HNA, respectively.

Conflict of interest

The authors declare no conflict of interest.

Acknowledgements

We thank the Integrated Laser Microscopy System and the Large-scale Protein Production System at the National Facility for Protein Science in Shanghai (NFPS), Shanghai Advanced Research Institute, Chinese Academy of Sciences, China, for technical support. We also thank the beamline BL18U1 of National Facility for Protein Science Shanghai (NFPS) at Shanghai Synchrotron Radiation Facility for their assistance in X-ray diffraction data collection. This work is supported by National Natural Science Foundation of China (No. 91957102) to Y.H. and we also thank the support from Innovative research team of high-level local universities in Shanghai (SHSMU-ZLCX20212601). .

References

1. Goldstein, J.L., et al., *Binding site on macrophages that mediates uptake and degradation of acetylated low density lipoprotein, producing massive cholesterol deposition.* Proceedings of the National Academy of Sciences, 1979. **76**(1): p. 333-7.
2. Brown, M.S. and J.L. Goldstein, *Receptor-mediated endocytosis: insights from the lipoprotein receptor system.* Proceedings of the National Academy of Sciences, 1979. **76**(7): p. 3330-7.
3. PrabhuDas, M.R., et al., *A Consensus Definitive Classification of Scavenger Receptors and Their Roles in Health and Disease.* J Immunol, 2017. **198**(10): p. 3775-3789.
4. Brown, M.S. and J.L. Goldstein, *Lipoprotein metabolism in the macrophage: implications for cholesterol deposition in atherosclerosis.* Annu Rev Biochem, 1983. **52**: p. 223-61.

5. Dunne, D.W., et al., *The type I macrophage scavenger receptor binds to gram-positive bacteria and recognizes lipoteichoic acid.* Proceedings of the National Academy of Sciences, 1994. **91**(5): p. 1863-7.
6. Krieger, M., et al., *Molecular flypaper, host defense, and atherosclerosis. Structure, binding properties, and functions of macrophage scavenger receptors.* J Biol Chem, 1993. **268**(7): p. 4569-72.
7. Means, T.K., et al., *Evolutionarily conserved recognition and innate immunity to fungal pathogens by the scavenger receptors SCARF1 and CD36.* J Exp Med, 2009. **206**(3): p. 637-53.
8. Cheng, C., et al., *The scavenger receptor SCARA1 (CD204) recognizes dead cells through spectrin.* J Biol Chem, 2019. **294**(49): p. 18881-18897.
9. Huang, L., et al., *SR-B1 drives endothelial cell LDL transcytosis via DOCK4 to promote atherosclerosis.* Nature, 2019. **569**(7757): p. 565-569.
10. Zani, I.A., et al., *Scavenger receptor structure and function in health and disease.* Cells, 2015. **4**(2): p. 178-201.
11. Yu, X., et al., *Scavenger Receptors: Emerging Roles in Cancer Biology and Immunology.* Advances in Cancer Research, 2015. **128**: p. 309-64.
12. Patten, D.A., et al., *Scavenger Receptors: Novel Roles in the Pathogenesis of Liver Inflammation and Cancer.* Semin Liver Dis, 2022. **42**(1): p. 61-76.
13. Wilkinson, K. and J. El Khoury, *Microglial scavenger receptors and their roles in the pathogenesis of Alzheimer's disease.* Int J Alzheimers Dis, 2012. **2012**: p. 489456.
14. Adachi, H., et al., *Expression cloning of a novel scavenger receptor from human endothelial cells.* J Biol Chem, 1997. **272**(50): p. 31217-20.
15. Tamura, Y., et al., *Scavenger receptor expressed by endothelial cells I (SREC-I) mediates the uptake of acetylated low density lipoproteins by macrophages stimulated with lipopolysaccharide.* J Biol Chem, 2004. **279**(30): p. 30938-44.
16. Apostolov, E.O., et al., *Scavenger receptors of endothelial cells mediate the*

uptake and cellular proatherogenic effects of carbamylated LDL. Arteriosclerosis Thrombosis and Vascular Biology, 2009. **29**(10): p. 1622-30.

17. Sano, M., et al., *N-glycans of SREC-I (scavenger receptor expressed by endothelial cells): essential role for ligand binding, trafficking and stability.* Glycobiology, 2012. **22**(5): p. 714-24.
18. Gong, J., et al., *T cell activation by heat shock protein 70 vaccine requires TLR signaling and scavenger receptor expressed by endothelial cells-1.* J Immunol, 2009. **183**(5): p. 3092-8.
19. Murshid, A., J. Gong, and S.K. Calderwood, *Heat shock protein 90 mediates efficient antigen cross presentation through the scavenger receptor expressed by endothelial cells-I.* J Immunol, 2010. **185**(5): p. 2903-17.
20. Murshid, A., J. Gong, and S.K. Calderwood, *Hsp90-peptide complexes stimulate antigen presentation through the class II pathway after binding scavenger receptor SREC-I.* Immunobiology, 2014. **219**(12): p. 924-31.
21. Jeannin, P., et al., *Complexity and complementarity of outer membrane protein A recognition by cellular and humoral innate immunity receptors.* Immunity, 2005. **22**(5): p. 551-60.
22. Beauvillain, C., et al., *The scavenger receptors SRA-1 and SREC-I cooperate with TLR2 in the recognition of the hepatitis C virus non-structural protein 3 by dendritic cells.* Journal of Hepatology, 2010. **52**(5): p. 644-51.
23. Ramirez-Ortiz, Z.G., et al., *The scavenger receptor SCARF1 mediates the clearance of apoptotic cells and prevents autoimmunity.* Nat Immunol, 2013. **14**(9): p. 917-26.
24. Ishii, J., et al., *SREC-II, a new member of the scavenger receptor type F family, trans-interacts with SREC-I through its extracellular domain.* J Biol Chem, 2002. **277**(42): p. 39696-702.
25. Patten, D.A., et al., *SCARF-1 promotes adhesion of CD4(+) T cells to human hepatic sinusoidal endothelium under conditions of shear stress.* Sci Rep, 2017. **7**(1): p. 17600.

26. Patten, D.A., et al., *Prognostic Value and Potential Immunoregulatory Role of SCARF1 in Hepatocellular Carcinoma.* Front Oncol, 2020. **10**: p. 565950.

27. Anastasio, N., et al., *Mutations in SCARF2 are responsible for Van Den Ende-Gupta syndrome.* Am J Hum Genet, 2010. **87**(4): p. 553-9.

28. Migliavacca, M.P., et al., *Sclerocornea in a patient with van den Ende-Gupta syndrome homozygous for a SCARF2 microdeletion.* American Journal of Medical Genetics, Part A 2014. **164a**(5): p. 1170-4.

29. Berwin, B., et al., *SREC-I, a type F scavenger receptor, is an endocytic receptor for calreticulin.* J Biol Chem, 2004. **279**(49): p. 51250-7.

30. Moriguchi, T., et al., *Ecrg4 peptide is the ligand of multiple scavenger receptors.* Sci Rep, 2018. **8**(1): p. 4048.

31. Pfistershammer, K., et al., *Identification of the scavenger receptors SREC-I, Cla-1 (SR-BI), and SR-AI as cellular receptors for Tamm-Horsfall protein.* Journal of Leukocyte Biology, 2008. **83**(1): p. 131-8.

32. Jorge, A.M., et al., *SCARF1-Induced Efferocytosis Plays an Immunomodulatory Role in Humans, and Autoantibodies Targeting SCARF1 Are Produced in Patients with Systemic Lupus Erythematosus.* J Immunol, 2022. **208**(4): p. 955-967.

33. Narazaki, M., M. Segarra, and G. Tosato, *Sulfated polysaccharides identified as inducers of neuropilin-1 internalization and functional inhibition of VEGF165 and semaphorin3A.* Blood, 2008. **111**(8): p. 4126-36.

34. Rechner, C., et al., *Host glycoprotein Gp96 and scavenger receptor SREC interact with PorB of disseminating Neisseria gonorrhoeae in an epithelial invasion pathway.* Cell Host Microbe, 2007. **2**(6): p. 393-403.

35. Schade, J. and C. Weidenmaier, *Cell wall glycopolymers of Firmicutes and their role as nonprotein adhesins.* FEBS Lett, 2016. **590**(21): p. 3758-3771.

36. Wicker-Planquart, C., et al., *Insights into the ligand binding specificity of SREC-II (scavenger receptor expressed by endothelial cells).* FEBS Open Bio, 2021. **11**(10): p. 2693-2704.

37. Nagase, T., et al., *Prediction of the coding sequences of unidentified human genes. XX. The complete sequences of 100 new cDNA clones from brain which code for large proteins in vitro.* DNA Res, 2001. **8**(2): p. 85-95.

38. Suzuki, E. and M. Nakayama, *The mammalian Ced-1 ortholog MEGF10/KIAA1780 displays a novel adhesion pattern.* Exp Cell Res, 2007. **313**(11): p. 2451-64.

39. Bork, P., et al., *Structure and distribution of modules in extracellular proteins.* Q Rev Biophys, 1996. **29**(2): p. 119-67.

40. Gillotte-Taylor, K., et al., *Scavenger receptor class B type I as a receptor for oxidized low density lipoprotein.* Journal of Lipid Research, 2001. **42**(9): p. 1474-1482.

41. Endemann, G., et al., *CD36 is a receptor for oxidized low density lipoprotein.* J Biol Chem, 1993. **268**(16): p. 11811-6.

42. Sawamura, T., et al., *An endothelial receptor for oxidized low-density lipoprotein.* Nature, 1997. **386**(6620): p. 73-7.

43. Cheng, C., et al., *Recognition of lipoproteins by scavenger receptor class A members.* J Biol Chem, 2021. **297**(2): p. 100948.

44. Shi, X., et al., *Characterization of residues and sequences of the carbohydrate recognition domain required for cell surface localization and ligand binding of human lectin-like oxidized LDL receptor.* J Cell Sci, 2001. **114**(Pt 7): p. 1273-82.

45. Ohki, I., et al., *Crystal structure of human lectin-like, oxidized low-density lipoprotein receptor 1 ligand binding domain and its ligand recognition mode to OxLDL.* Structure, 2005. **13**(6): p. 905-17.

46. Kar, N.S., et al., *Mapping and characterization of the binding site for specific oxidized phospholipids and oxidized low density lipoprotein of scavenger receptor CD36.* J Biol Chem, 2008. **283**(13): p. 8765-71.

47. Terwilliger, T.C., et al., *AlphaFold predictions are valuable hypotheses, and accelerate but do not replace experimental structure determination.* bioRxiv,

2023.

48. Wicker-Planquart, C., et al., *Molecular and Cellular Interactions of Scavenger Receptor SR-F1 With Complement C1q Provide Insights Into Its Role in the Clearance of Apoptotic Cells.* Front Immunol, 2020. **11**: p. 544.

49. Dolinsky, T.J., et al., *PDB2PQR: an automated pipeline for the setup of Poisson-Boltzmann electrostatics calculations.* Nucleic Acids Res, 2004. **32**(Web Server issue): p. W665-7.

50. Holzl, M.A., et al., *The zymogen granule protein 2 (GP2) binds to scavenger receptor expressed on endothelial cells I (SREC-I).* Cell Immunol, 2011. **267**(2): p. 88-93.

51. Baur, S., et al., *A nasal epithelial receptor for Staphylococcus aureus WTA governs adhesion to epithelial cells and modulates nasal colonization.* PLoS Pathog, 2014. **10**(5): p. e1004089.

52. Murshid, A., T.J. Borges, and S.K. Calderwood, *Emerging roles for scavenger receptor SREC-I in immunity.* Cytokine, 2015. **75**(2): p. 256-60.

53. Patten, D.A., *SCARF1: a multifaceted, yet largely understudied, scavenger receptor.* Inflammation Research, 2018. **67**(8): p. 627-632.

54. Li, Z., et al., *Recognition of EGF-like domains by the Notch-modifying O-fucosyltransferase POFUT1.* Nat Chem Biol, 2017. **13**(7): p. 757-763.

55. Singh, B., G. Carpenter, and R.J. Coffey, *EGF receptor ligands: recent advances.* F1000Res, 2016. **5**.

56. Ohlin, A.K., S. Linse, and J. Stenflo, *Calcium binding to the epidermal growth factor homology region of bovine protein C.* J Biol Chem, 1988. **263**(15): p. 7411-7.

57. Dahlbäck, B., B. Hildebrand, and S. Linse, *Novel type of very high affinity calcium-binding sites in beta-hydroxyasparagine-containing epidermal growth factor-like domains in vitamin K-dependent protein S.* The Journal of biological chemistry, 1990. **265 30**: p. 18481-9.

58. Stenflo, J., Y. Stenberg, and A. Muranyi, *Calcium-binding EGF-like modules*

in coagulation proteinases: function of the calcium ion in module interactions. Biochim Biophys Acta, 2000. **1477**(1-2): p. 51-63.

59. Malinauskas, T., et al., *Modular mechanism of Wnt signaling inhibition by Wnt inhibitory factor 1.* Nat Struct Mol Biol, 2011. **18**(8): p. 886-93.

60. Ishigaki, T., et al., *Purification, crystallization and preliminary X-ray analysis of the ligand-binding domain of human lectin-like oxidized low-density lipoprotein receptor 1 (LOX-1).* Acta Crystallogr Sect F Struct Biol Cryst Commun, 2005. **61**(Pt 5): p. 524-7.

61. Febbraio, M., D.P. Hajjar, and R.L. Silverstein, *CD36: a class B scavenger receptor involved in angiogenesis, atherosclerosis, inflammation, and lipid metabolism.* J Clin Invest, 2001. **108**(6): p. 785-91.

62. Park, H., F.G. Adsit, and J.C. Boyington, *The 1.4 angstrom crystal structure of the human oxidized low density lipoprotein receptor lox-1.* J Biol Chem, 2005. **280**(14): p. 13593-9.

63. Gaidukov, L., et al., *Glycine Dimerization Motif in the N-terminal Transmembrane Domain of the High Density Lipoprotein Receptor SR-BI Required for Normal Receptor Oligomerization and Lipid Transport.* Journal of Biological Chemistry, 2011. **286**(21): p. 18452-18464.

64. Zhang, R., et al., *The Role of SREC-I in Innate Immunity to Aspergillus fumigatus Keratitis.* Invest Ophthalmol Vis Sci, 2021. **62**(9): p. 12.

65. Minor, W., et al., *HKL-3000: the integration of data reduction and structure solution--from diffraction images to an initial model in minutes.* Acta Crystallogr D Biol Crystallogr, 2006. **62**(Pt 8): p. 859-66.

66. Liebschner, D., et al., *Macromolecular structure determination using X-rays, neutrons and electrons: recent developments in Phenix.* Acta Crystallogr D Struct Biol, 2019. **75**(Pt 10): p. 861-877.

67. McCoy, A.J., et al., *Phaser crystallographic software.* J Appl Crystallogr, 2007. **40**(Pt 4): p. 658-674.

68. Emsley, P. and K. Cowtan, *Coot: model-building tools for molecular graphics.*

Acta Crystallogr D Biol Crystallogr, 2004. **60**(Pt 12 Pt 1): p. 2126-32.

69. Afonine, P.V., et al., *Towards automated crystallographic structure refinement with phenix.refine.* Acta Crystallogr D Biol Crystallogr, 2012. **68**(Pt 4): p. 352-67.

70. Williams, C.J., et al., *MolProbity: More and better reference data for improved all-atom structure validation.* Protein Sci, 2018. **27**(1): p. 293-315.

71. Pettersen, E.F., et al., *UCSF Chimera--a visualization system for exploratory research and analysis.* J Comput Chem, 2004. **25**(13): p. 1605-12.

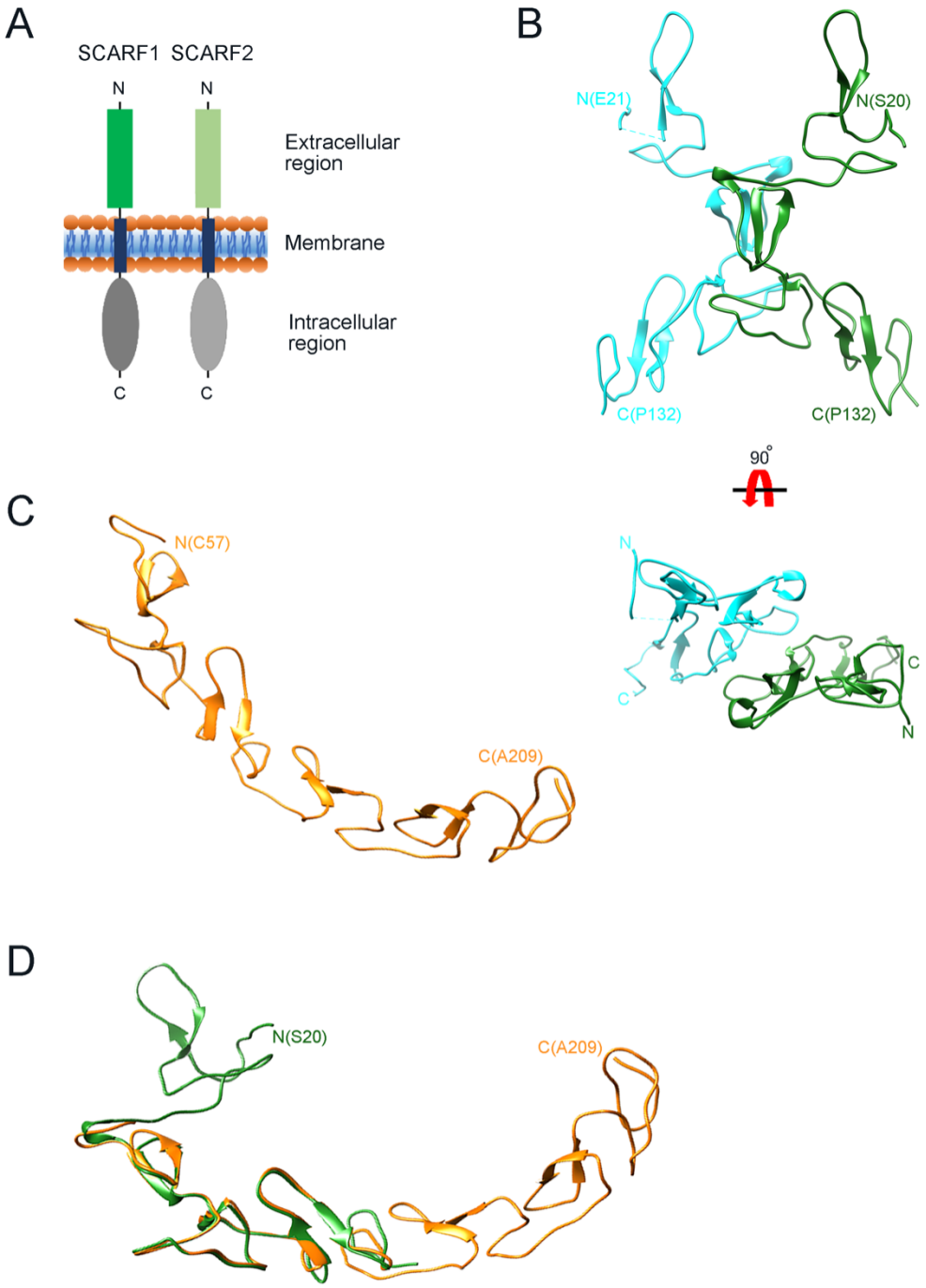
A
SCARF1 SCARF2
N
N
Extracellular region
Membrane
Intracellular region
C
C
B
N(E21)
N(S20)
C(P132)
C(P132)
90°
N
C
C
N
C
N(C57)
C(A209)
D
N(S20)
C(A209)

Figure 1. Crystal structure of the N-terminal fragments of SCARF1

(A) A schematic model of human SCARF1 and SCARF2.

(B) Ribbon diagrams of a homodimer of an N-terminal fragment (f1, 20-132 aa; two monomers are shown in cyan and green, respectively) of SCARF1.

(C) A ribbon diagram of an N-terminal fragment (f2, 57-209 aa, gold) of SCARF1.

(D) Structure of the N-terminal fragment of SCARF1 (20-209 aa) by superimposing the crystal structures of f1 (green) and f2 (gold).

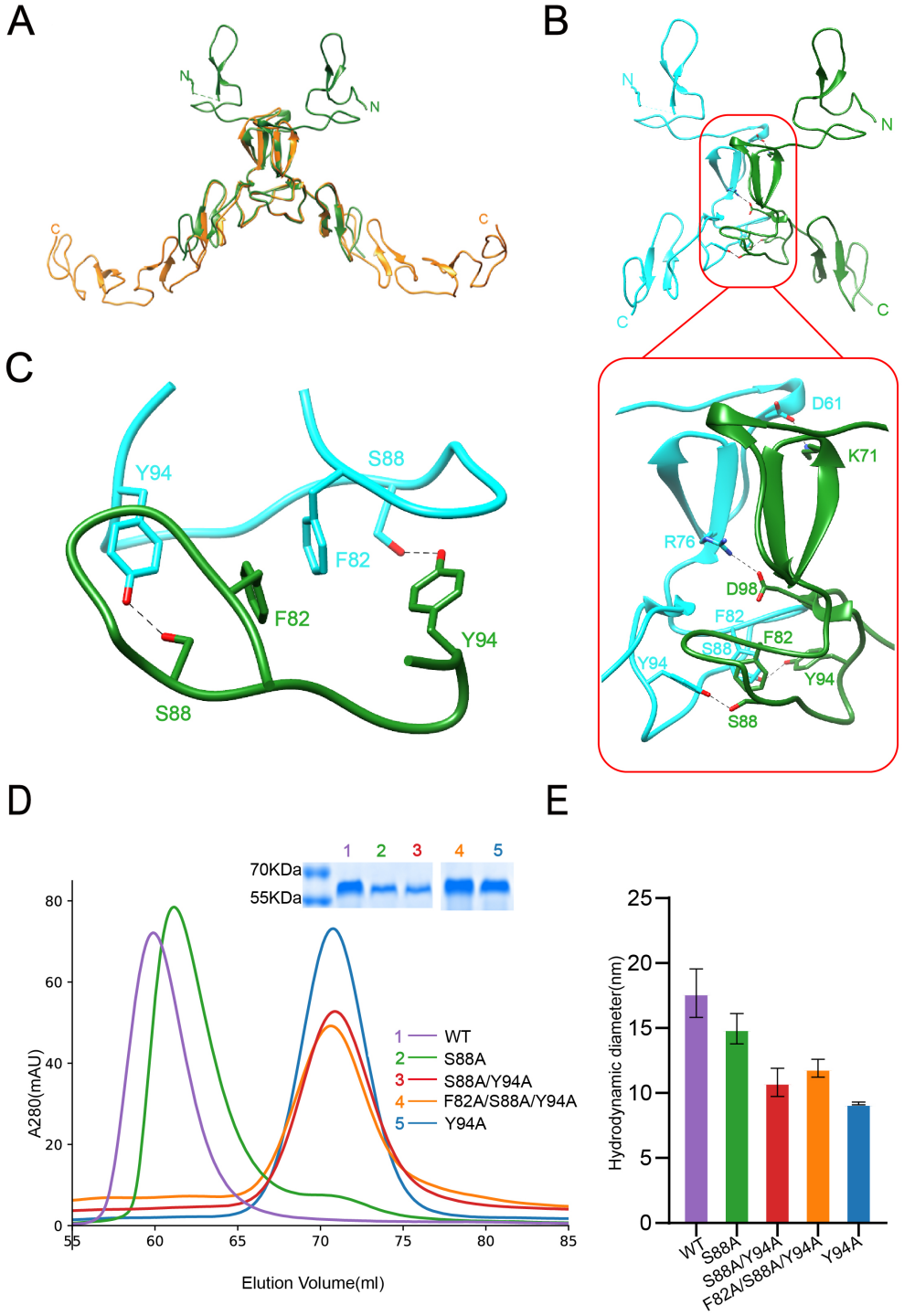
A
N
N
C
C
B
N
N
C
C
D61
K71
R76
D98
F82
F82
S88
Y94
Y94
S88
C
Y94
S88
F82
F82
Y94
S88
D
70KDa
55KDa
1
2
3
4
5
A280(mAU)
Elution Volume(ml)
1 WT
2 S88A
3 S88A/Y94A
4 F82A/S88A/Y94A
5 Y94A
E
Hydrodynamic diameter(nm)
WT
S88A
S88A/Y94A
F82A/S88A/Y94A
Y94A

Figure 2. Dimerization of SCARF1

(A) Superposition of the homodimers of f1 (green) and f2 (gold) in the crystals.

(B) The dimeric interface of f1 fragment of SCARF1 (red rectangles). Two monomers are colored in cyan and green, respectively. The side chains of the residues that form hydrogen bonds (dashed lines), salt bridges (dashed lines) and π-π interactions are labeled.

(C) A local view of the dimeric interface of SCARF1. The side chains of the residues that form hydrogen bonds (dashed lines) and π-π interactions are labeled.

(D) The SEC profiles of the wild type and the mutants of SCARF1 ectodomain. The SDS-PAGE of the peak fraction of each SEC profile is also shown.

(E) The hydrodynamic diameters of the wild type and the mutants of SCARF1 ectodomain measured by DLS.

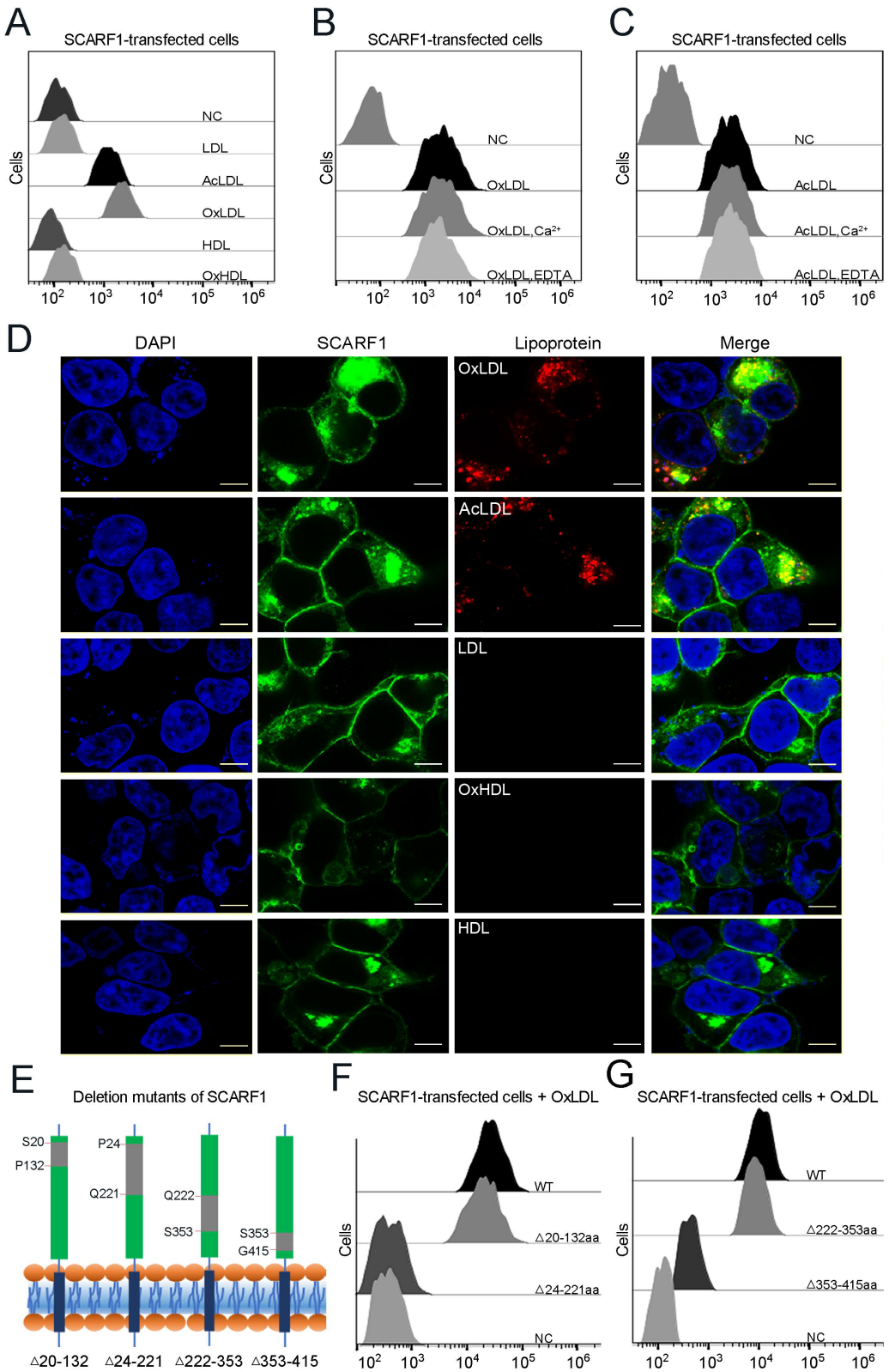
A
SCARF1-transfected cells
Cells
NC
LDL
AcLDL
OxLDL
HDL
OxHDL
B
SCARF1-transfected cells
NC
OxLDL
OxLDL,Ca2+
OxLDL,EDTA
C
SCARF1-transfected cells
NC
AcLDL
AcLDL,Ca2+
AcLDL,EDTA
D
DAPI
SCARF1
Lipoprotein
Merge
OxLDL
AcLDL
LDL
OxHDL
HDL
E
Deletion mutants of SCARF1
S20
P132
P24
Q221
Q222
S353
S353
G415
Δ20-132
Δ24-221
Δ222-353
Δ353-415
F
SCARF1-transfected cells + OxLDL
WT
Δ20-132aa
Δ24-221aa
NC
G
SCARF1-transfected cells + OxLDL
WT
Δ222-353aa
Δ353-415aa
NC

Figure 3. SCARF1 recognizes the modified LDLs

(A) Interactions of LDL, AcLDL, OxLDL, HDL and OxHDL with the SCARF1-transfected cells by flow cytometry (NC represents the non-transfected cells).

(B) Interactions of OxLDL with the SCARF1-transfected cells in the presence of Ca^{2+} or EDTA by flow cytometry.

(C) Interactions of AcLDL with the SCARF1-transfected cells in the presence of Ca^{2+} or EDTA by flow cytometry.

(D) Confocal fluorescent images of the SCARF1-transfected cells incubated with OxLDL, AcLDL, LDL, OxHDL or HDL (scale bar, 7.5 μm).

(E) Schematic diagrams of the deletion mutants of SCARF1. The deleted regions are labeled and shown in gray.

(F) Interactions of OxLDL with the deletion mutants $SCARF1^{\Delta 20\text{-}132aa}$ and $SCARF1^{\Delta 24\text{-}221aa}$ by flow cytometry

(G) Interactions of OxLDL with the deletion mutants $SCARF1^{\Delta 222\text{-}353aa}$ and $SCARF1^{\Delta 353\text{-}415aa}$ by flow cytometry

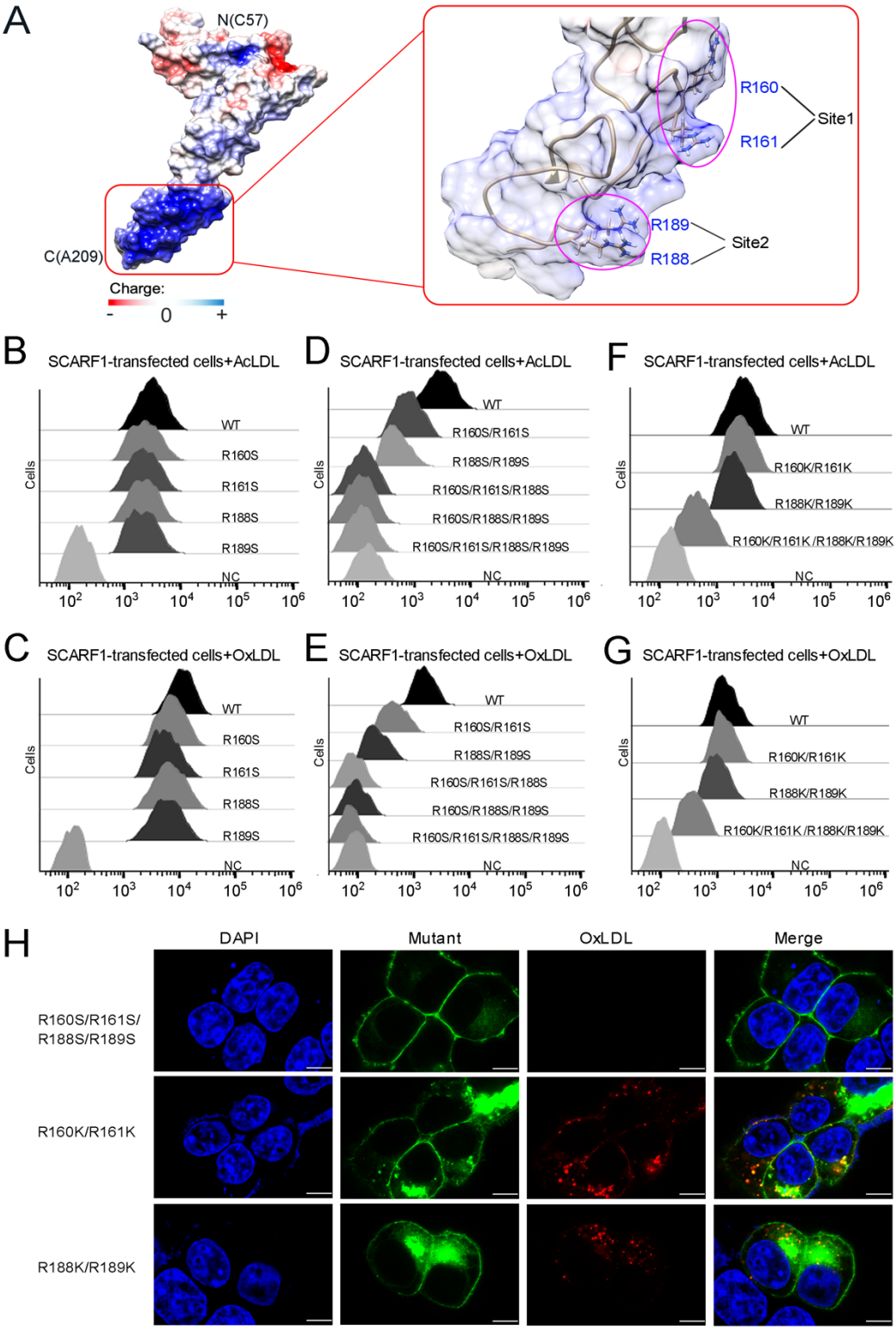
A
N(C57)
C(A209)
Charge:
- 0 +
R160
R161
Site1
R189
R188
Site2
B
SCARF1-transfected cells+AcLDL
WT
R160S
R161S
R188S
R189S
NC
Cells
D
SCARF1-transfected cells+AcLDL
WT
R160S/R161S
R188S/R189S
R160S/R161S/R188S
R160S/R188S/R189S
R160S/R161S/R188S/R189S
NC
F
SCARF1-transfected cells+AcLDL
WT
R160K/R161K
R188K/R189K
R160K/R161K /R188K/R189K
NC
C
SCARF1-transfected cells+OxLDL
E
SCARF1-transfected cells+OxLDL
G
SCARF1-transfected cells+OxLDL
H
DAPI
Mutant
OxLDL
Merge
R160S/R161S/
R188S/R189S
R160K/R161K
R188K/R189K

Figure 4. The binding sites of modified LDLs on SCARF1

(A) Surface electrostatic potential of f2 fragment shows a positively charged region on SCARF1 (left, red rectangle), which contains four arginines at site 1 and site 2 (right, magenta ovals).

(B) Interactions of AcLDL with the cells transfected with the single mutants (R to S) of the binding sites by flow cytometry.

(C) Interactions of OxLDL with the cells transfected with the single mutants (R to S) of the binding sites by flow cytometry.

(D) Interactions of AcLDL with the cells transfected with the double, triple or quadruple mutants (R to S) of the binding sites by flow cytometry.

(E) Interactions of OxLDL with the cells transfected with the double, triple or quadruple mutants (R to S) of the binding sites by flow cytometry.

(F) Interactions of AcLDL with the cells transfected with the double or quadruple mutants (R to K) of the binding sites by flow cytometry.

(G) Interactions of OxLDL with the cells transfected with the double or quadruple mutants (R to K) of the binding sites by flow cytometry.

(H) Confocal fluorescent images of the SCARF1 mutant transfected cells incubated with OxLDL (scale bar, 7.5 μm).

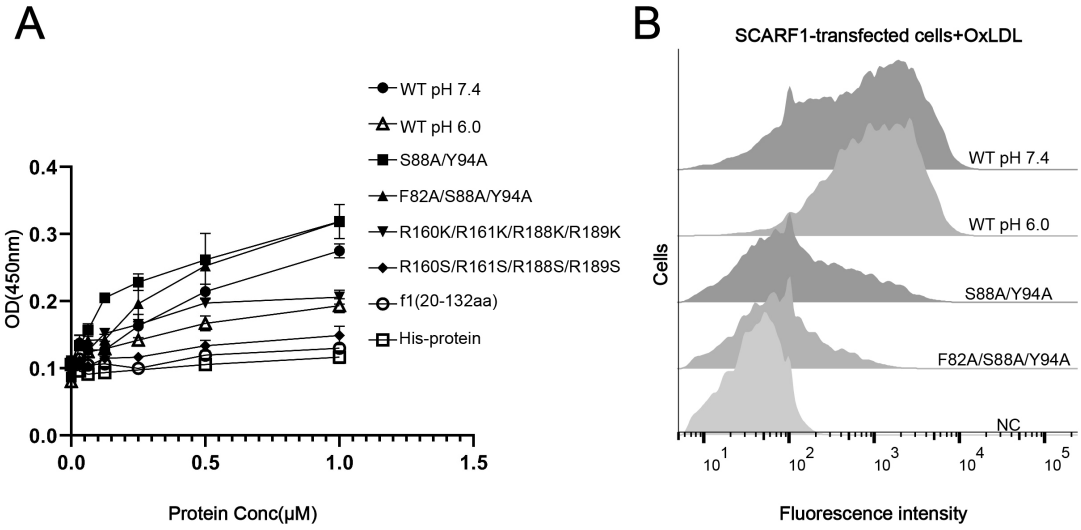

Figure 5. The binding of SCARF1 with OxLDL

(A) ELISA of the interactions of OxLDL with the wild type and the mutants of the ectodomain of SCARF1(f1 fragment is also applied). The assays are performed at pH 7.4 if not labeled. The ectodomain of human HER3 (His-protein) is applied as a control.

(B) Interactions of OxLDL with the cells transfected with the wild type and the mutants of SCARF1 by flow cytometry. The assays are performed at pH 7.4 if not labeled.

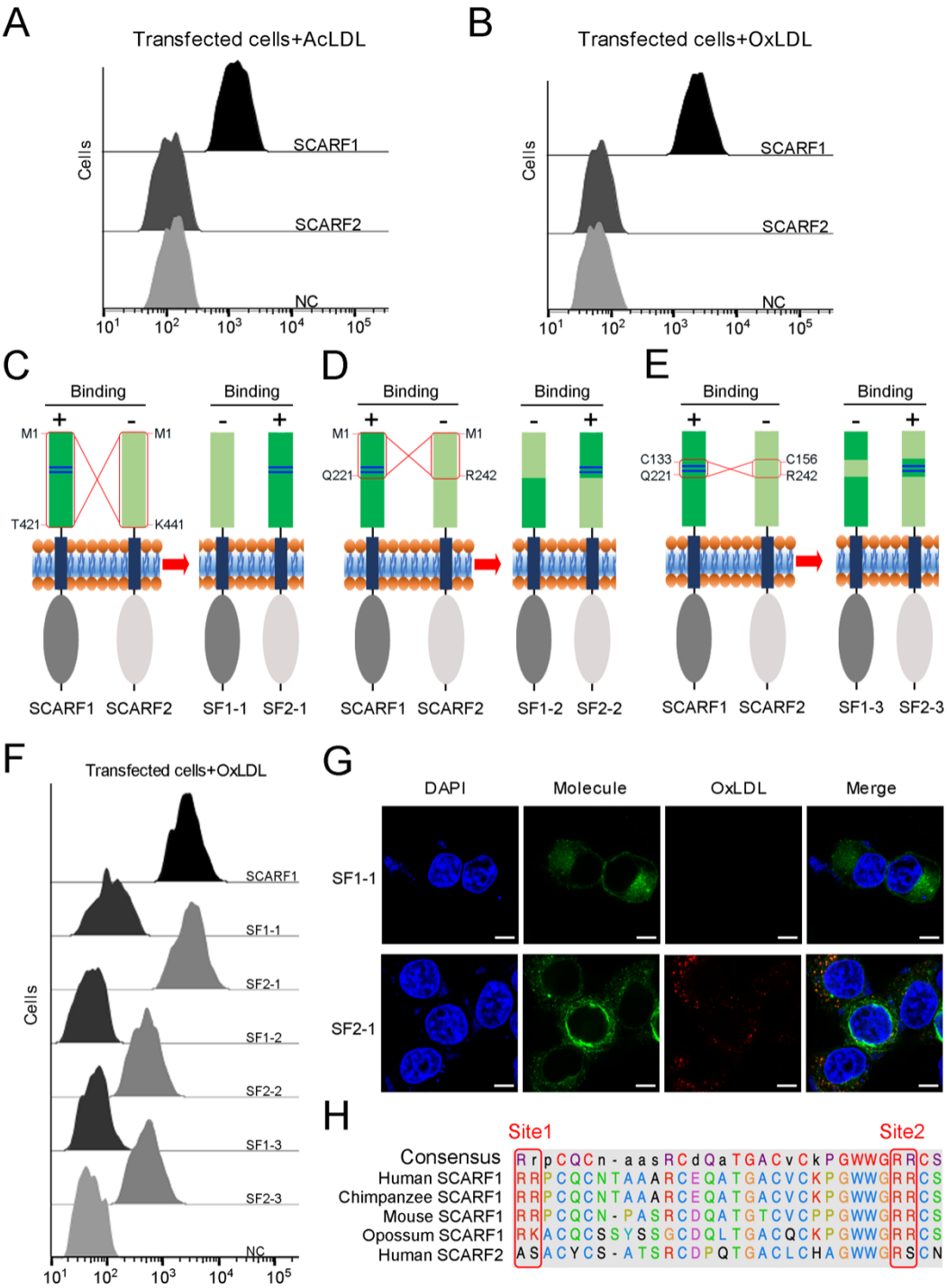
A
Transfected cells+AcLDL
Cells
SCARF1
SCARF2
NC
B
Transfected cells+OxLDL
C
Binding
M1
T421
K441
SCARF1 SCARF2 SF1-1 SF2-1
D
Q221
R242
SF1-2 SF2-2
E
C133
C156
SF1-3 SF2-3
F
SF1-1
SF2-1
SF1-2
SF2-2
SF1-3
SF2-3
G
DAPI
Molecule
OxLDL
Merge
H
Site1
Site2
Consensus
Human SCARF1
Chimpanzee SCARF1
Mouse SCARF1
Opossum SCARF1
Human SCARF2

Figure 6. The interactions of modified LDLs with SCARF1-SCARF2 chimeric molecules

(A) Interaction of AcLDL with the SCARF1 or SCARF2 transfected cells by flow cytometry.

(B) Interaction of OxLDL with the SCARF1 or SCARF2 transfected cells by flow cytometry.

(C), (D) and (E) Schematic diagrams of the SCARF1-SCARF2 chimeric molecules generated for binding assays. The switched regions are indicated by red rectangles. The positively charged site 1 and site 2 of SCARF1 are shown as blue lines. The binding of molecules with OxLDL is indicated as + (positive) or – (negative).

(F) Interactions of OxLDL with the chimeric molecule transfected cells by flow cytometry.

(G) Confocal fluorescent images of the chimera molecule SF1-1 or SF2-1 transfected cells incubated with OxLDL (scale bar, 7.5 μm).

(H) Sequence alignment of the binding sites of SCARF1 from different species and human SCARF2.

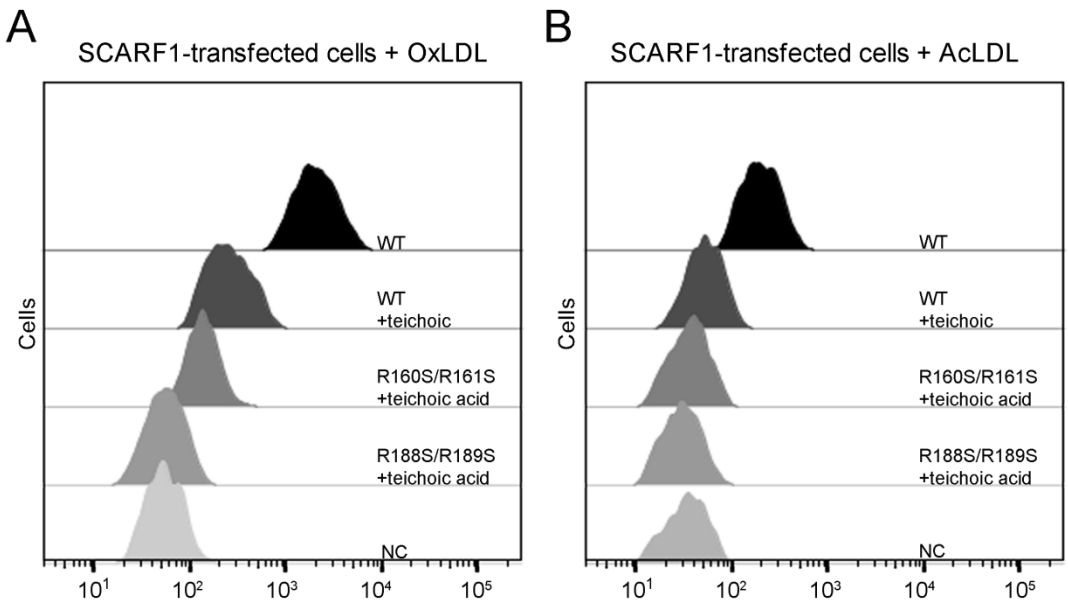

Figure 7. Inhibition of the interactions of SCARF1 with modified LDLs by teichoic acids

(A) Interaction of OxLDL with the cells transfected with the wild type or mutants of SCARF1 in the presence of teichoic acids by flow cytometry.

(B) Interaction of AcLDL with the cells transfected with the wild type or mutants of SCARF1 in the presence of teichoic acids by flow cytometry.

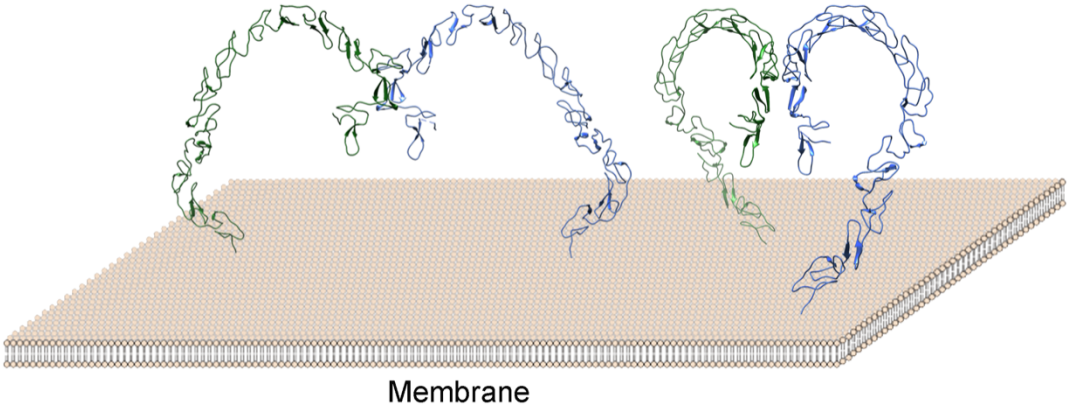

Figure 8. A model of the SCARF1 homodimers on the membrane surface.

The structure of the SCARF1 homodimer is generated by combining the crystal structures of f1 and f2, and rest of the ectodomain is from AlphaFold prediction. The monomers are colored in green or blue.

Supplementary Figures

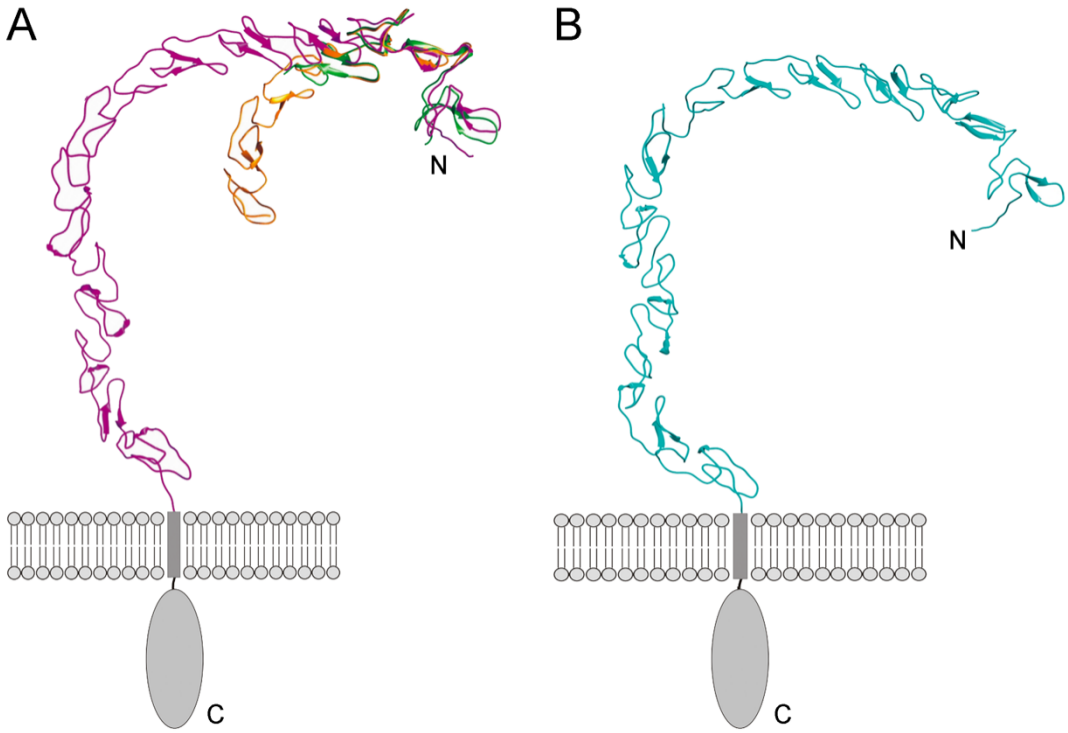

Figure S1. Models of the ectodomains of SCARF1 and SCARF2 by AlphaFold.

(A) Superposition of the crystal structures of f1 (green) and f2 (gold) with the AlphaFold model of the SCARF1 ectodomain (magenta).

(B) AlphaFold model of the SCARF2 ectodomain (cyan).

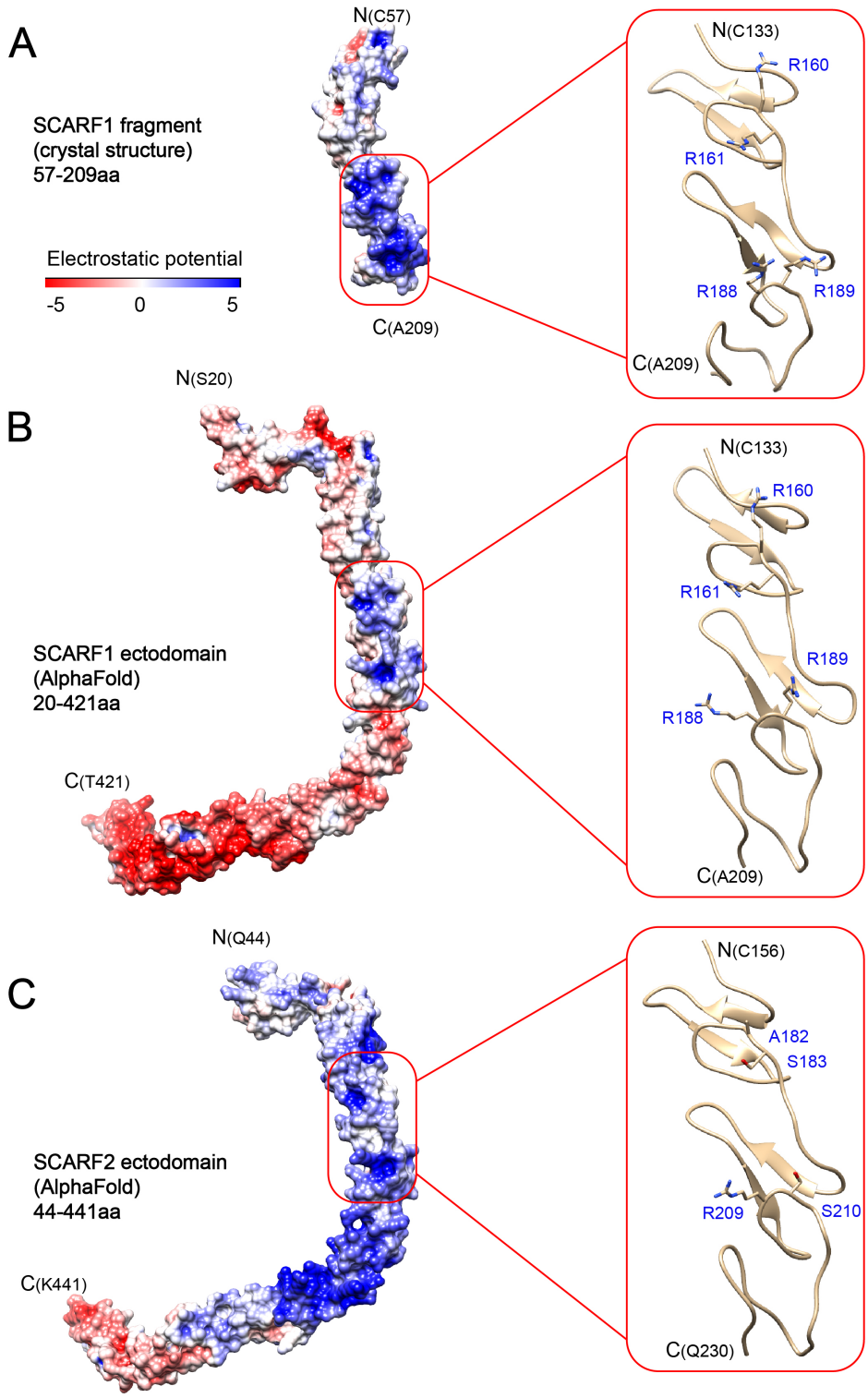
A
SCARF1 fragment
(crystal structure)
57-209aa
Electrostatic potential
-5
0
5
N(C57)
C(A209)
N(C133)
R160
R161
R188
R189
C(A209)
B
N(S20)
SCARF1 ectodomain
(AlphaFold)
20-421aa
C(T421)
N(C133)
R160
R161
R189
R188
C(A209)
C
N(Q44)
SCARF2 ectodomain
(AlphaFold)
44-441aa
C(K441)
N(C156)
A182
S183
R209
S210
C(Q230)

Figure S2. Surface electrostatic potential of SCARF1 and SCARF2

(A) Surface electrostatic potential of the crystal structure of a SCARF1 fragment (57-209 aa). A ribbon diagram of the region around the lipoprotein binding site (red rectangle) is shown on the right. The side chains of the arginines are also shown.

(B) Surface electrostatic potential of the ectodomain of SCARF1 from AlphaFold. A ribbon diagram of the region around the lipoprotein binding site (red rectangle) is shown on the right. The side chains of the arginines are also shown.

(C) Surface electrostatic potential of the ectodomain of SCARF2 from AlphaFold. A ribbon diagram of the corresponding region of SCARF1 lipoprotein binding site (red rectangle) is shown on the right. The side chains of the corresponding residues are also shown.

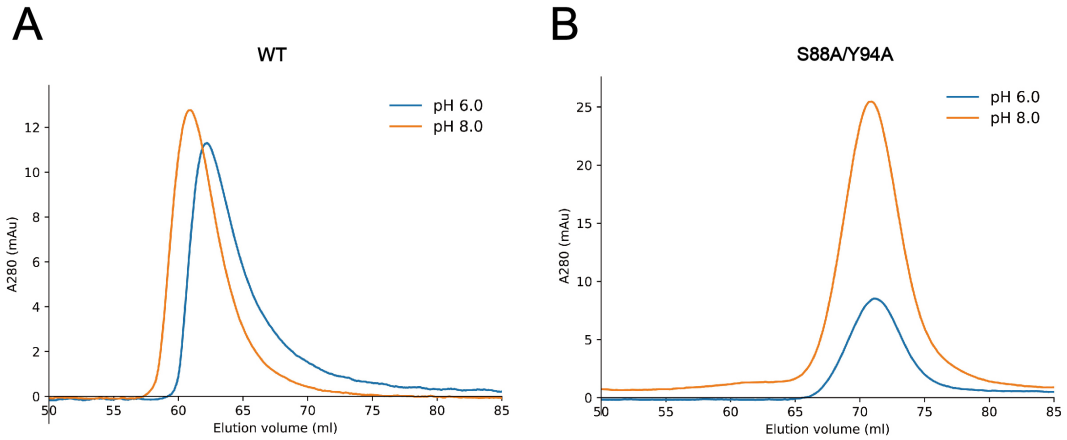

Figure S3. The SEC profiles of the ectodomain of SCARF1

(A) The SEC profiles of the wild type ectodomain of SCARF1 at pH 6.0 or pH 8.0

(B) The SEC profiles of a monomeric mutant of the ectodomain of SCARF1 at pH 6.0 or pH 8.0

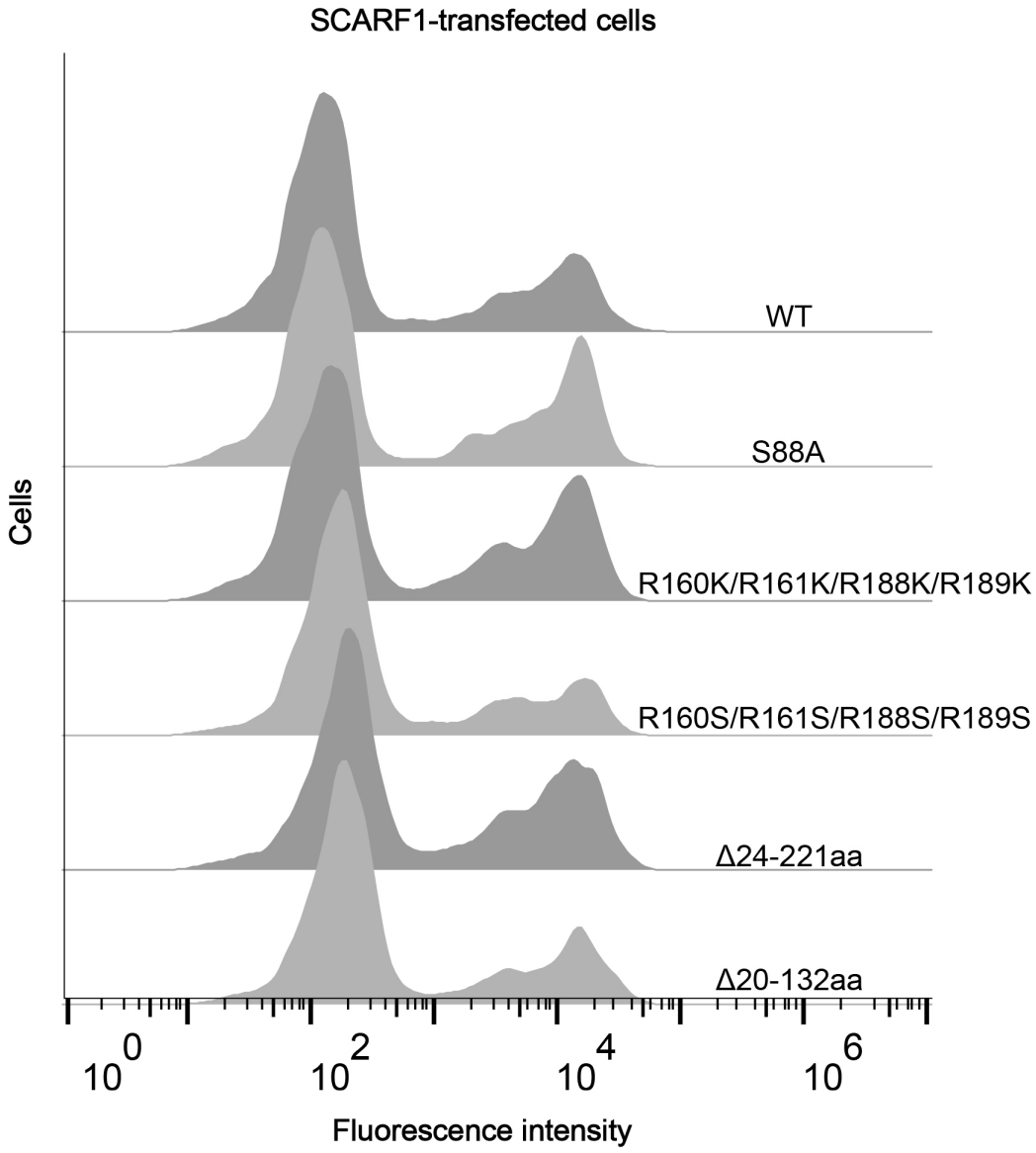

Figure S4. The expression of SCARF1 and mutants on the cell surface.

The expression of SCARF1 and mutants on the cell surface are monitored by flow cytometry using anti-SCARF1 antibody.

Table S1. X-ray data collection and processing

Protein	20-132aa of SCARF1	20-221aa of SCARF1
Beamline	SSRF BL18U1	SSRF BL18U1
Wavelength (Å)	0.98	0.98
Space group	$P2_12_12_1$	$P4_122$
Cell parameters		
a, b, c (Å)	47.01, 50.70, 110.74	102.01, 102.01, 83.61
α, β, γ (°)	90, 90, 90	90, 90, 90
Resolution (Å)	30.00-2.10	30.00-2.60
	(2.18-2.10)	(2.69-2.60)
R_{merge}	0.075(0.398)	0.088(0.795)
R_{pim}	0.023(0.149)	0.018(0.176)
Unique reflections	16105(1567)	14015(1299)
I/σ (I)	33(3.03)	45.5(2.75)
Completeness (%)	99.9(94.6)	99.2(93.4)
Multiplicity	9.9(7.5)	23.3(17.9)

Values in parentheses are for the highest-resolution shell.

Table S2. Crystallographic statistics of the structures

Protein	20-132aa of SCARF1	20-221aa of SCARF1
Resolution (Å)	24.71-2.20(2.28-2.20)	26.89-2.60(2.69-2.60)
R_{work}	0.219(0.244)	0.229(0.339)
R_{free}	0.252(0.292)	0.246(0.347)
Protein atoms	3223	1133
Wilson B-factor ($Å^2$)	38.8	71.2
Average B, all atoms ($Å^2$)	56.0	86.0
Rmsd bonds (Å)	0.36	0.43
Rmsd angles (°)	0.60	0.71
Ramachandran favored (%)	95.41	95.36
Ramachandran outliers (%)	0	0
PDB code	8HN0	8HNA

Values in parentheses are for the highest-resolution shell.